# Suppression of the B-mode in SC-Cuts

E. P. EerNisse and D. Puccio
Quartzdyne, Inc.
Salt Lake City, USA

***Abstract*—We have found it possible to suppress the B-mode of fundamental mode SC-cuts over wide temperature ranges by imbedding the B-mode in a cluster of C-mode anharmonics with choice of diopter. This work presents a variety of theoretical results and experimental data supporting the approach.**

## I. INTRODUCTION

Ever since the advent of the SC-cut [1,2], users have had to deal with the B-mode (fast-shear mode), which is piezoelectrically as active as the C-mode (slow-shear mode). If one desires to use only the C-mode of the SC-cut, one must suppress the B-mode, either by crystal design, or by circuit techniques. Early work on suppression of the B-mode in fundamental mode SC-cuts showed that choice of diopter and orientation of the mounts helped [3]. A recent publication [4] demonstrated that the motional capacitance of the fundamental B-mode of a 3rd overtone crystal design is affected by diopter choice because the B-mode interacts with C-mode anharmonics. This work expands that result to accomplish suppression of the B-mode in fundamental mode SC-cuts by crystal design.

The use of the SC-cut in an oscillator circuit as a reference signal for electronic applications in the down-hole environment of the oil and gas industry offers the advantages of superior ageing and well-behaved frequency vs. temperature characteristics. However, the size must be small, which suggests using the fundamental C-mode, and the oscillator circuit must reliably start up on the correct crystal mode in temperature ranges that can be as large as from -40 C to 225 C. Inductors are one of the most unreliable circuit components in the high temperatures and high shocks encountered in this environment, so suppression of the B-mode with crystal design is preferred rather than with circuit design. This work demonstrates successful suppression of the B-mode in fundamental mode SC-cut crystals by judicious choice of diopter.

## II. THEORETICAL DEVELOPMENT

### *A. Analytical modeling*

Analyses of the C-mode and B-mode families with published analytical models built on the work of Stevens and Tiersten [5-7] lack the ability to characterize coupling between the C-mode and the B-mode because a number of terms involving second-order derivatives and products of derivatives in the in-plane coordinate directions are left out of the theory. However, useful results may be obtained with these models. Two different fundamental mode, plano-convex, crystal designs will be discussed here, 0.635 cm diameter at 7.2 MHz and 1.08 cm diameter at 3.6864 MHz.

Figure 1 shows analytical model results for the 7.2 MHz design as frequency, $f$, vs. diopter, $D$. The range of $D$ was chosen to adequately trap the C-mode but still leave a reasonable thickness at the blank edge. The mode designations used here are $C_{1mp}$ for the C-modes, with $C_{100}$ being the fundamental C-mode, and $m + p = 2$ *or* $4$ being the relevant anharmonic mode families with symmetry that might couple to the B-mode, $B_{100}$. Note in Fig. 1 that there is a considerable range of $D$ where the B-mode frequency is embedded within the $m + p = 4$ C-mode anharmonic family. The results in Fig. 1 are for temperature, $T$, at 25 C. Since the B-mode has a large negative $f$ vs. $T$ slope, as $T$ increases, the B-mode will be moving down in frequency relative to the C-mode anharmonic family. This can be pictured in Fig. 1 by observing that increasing $T$ has the same effect as $D$ becoming larger. Thus, it is desirable to use a $D$ value that is small enough to leave the B-mode embedded within the C-mode anharmonic family at the highest $T$ to be encountered in use.

Figure 2 shows similar results for the analytical modeling of the 3.6864 MHz design.

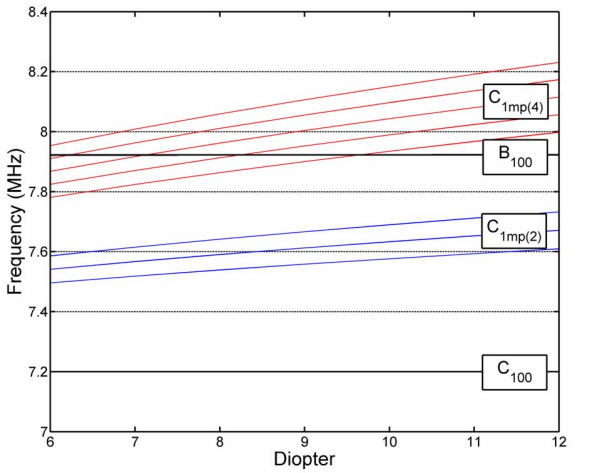


Figure 1. *Analytical frequency vs. Diopter: 7.2 MHz blank design.*

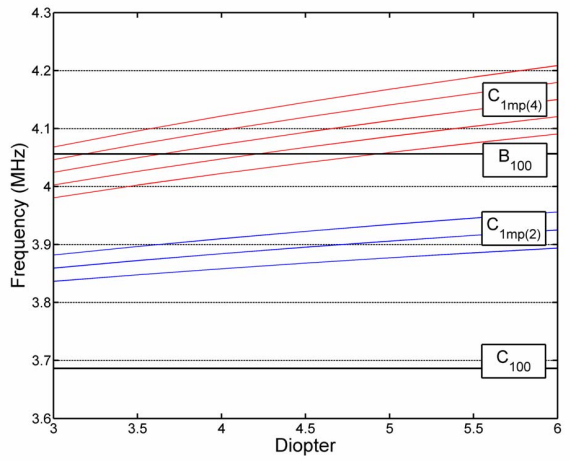


Figure 2. *Analytical frequency vs. Diopter: 3.6864 MHz blank design.*

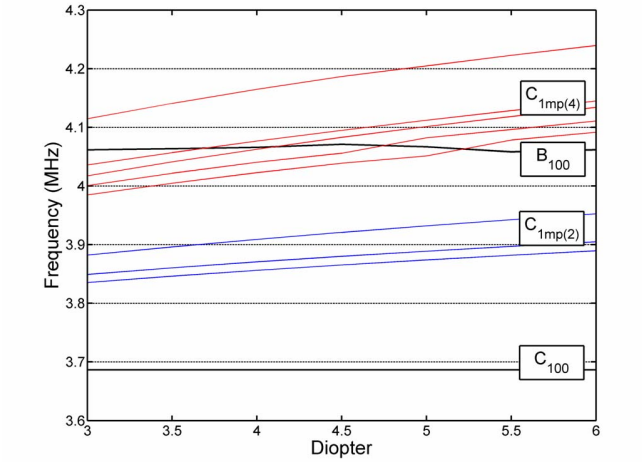


Figure 3. *Variational frequency vs. Diopter: 3.6864 MHz blank design.*

## *B. Variational modeling*

For some time, the Calculus of Variations has been used to model resonant modes in a crystal [4,8,9]. This approach includes the coupling between the B-mode and the C-modes [4]. We use the conventional *yxwl(ϕθ)* blank designation with $x_2$ the blank normal and $x_1$, $x_3$ the in-plane axes. Figure 3 shows variational results for the 3.6864 MHz design as frequency vs. diopter. Although the results in Fig. 3 look similar to those in Fig. 2, there is an important difference. The B-mode frequency and the $m + p = 4$ C-mode frequencies are perturbed by the presence of each other.

Although the frequency perturbations are small on the scale shown in Fig. 3, the impact on their mode shapes is dramatic. So dramatic, in many cases, that it is difficult to apply a $B_{100}$ identification to any one of the calculated modes. This is seen in Fig. 4, where filled-contour plots of the displacement component $u_3$ in the $x_3$ direction (typically thought of as the fast-shear displacement direction) are shown for the mode with the largest $u_3$ displacement value for four different $D$ values for the 3.6864 MHz blank design.

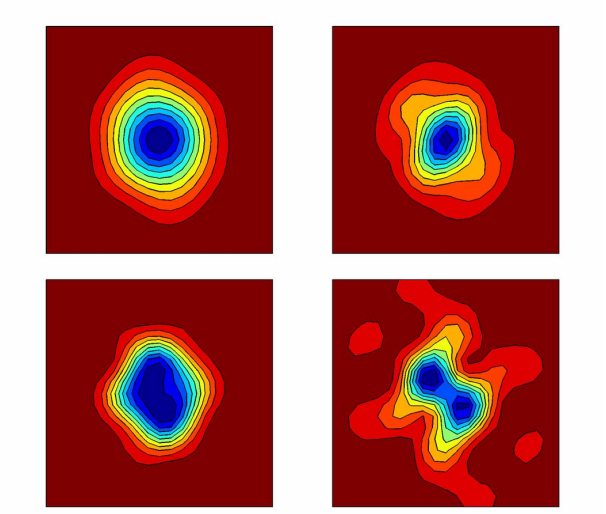

Figure 4. *Variational mode shapes for the B-mode $u_3$ displacement for the 3.6864 MHz blank design, D values clockwise from the upper left are D= 3,4,5,6. Each plot area is 1.0 cm on a side.*

Note that for the smallest and largest $D$ values the mode shape is reasonably well-trapped because the B-mode is outside the four closely grouped members of the $m + p = 4$ C-mode anharmonics (see Fig. 3). In contrast, for the in-between $D$ values, the mode shapes are distorted because the B-mode is close to an $m + p = 4$ C-mode anharmonic.

It should be noted here that the variational modeling involves using basis functions that are close to the analytical solutions [4], and that the integrations used in constructing the models extend to infinity. Thus, the calculated mode shapes can extend beyond the blank edges.

Figure 5 shows why it is difficult to identify the B-mode when it couples to the C-mode anharmonics. In Fig. 5, filled-contour mode shapes for $u_3$ are shown for some of the modes near where the B-mode should appear for the 3.6864 blank design for $D = 5$. Note in Fig. 5 that there is a strong component of the B-mode deflection component for three different modes.

There are two main impacts of the $B_{100}$ mode distortions caused by coupling to C-mode anharmonics. The motional capacitance is reduced, and the mode shape is not as well trapped. The major impact on the motional resistance of the B-mode is a drop in its $Q$ due to the mode being spread out to the edges of the blank. The mode shapes in Figs. 4 and 5 for the $u_3$ component of the displacement show only part of the picture. The strong coupling to the C-mode anharmonics of $m + p = 4$ also includes spread-out displacement shapes for the $u_1$ displacement component in the $x_1$ direction (typically thought of as the slow shear mode displacement direction). Figure 6 shows calculated results for this displacement component for the 3.6864 MHz blank design with the $D$ values from Fig. 4. Note that the magnitudes of these displacements are relatively spread out.

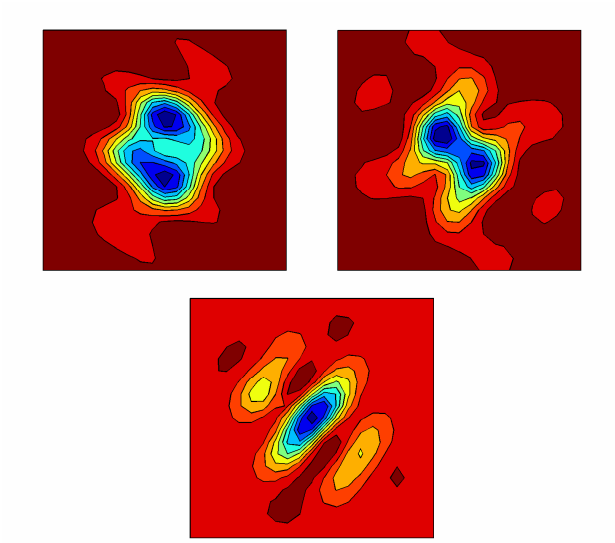

Figure 5. *Mode shapes for the $u_3$ displacement for three modes near where the B-mode should appear for the 3.6864 MHz blank design for D=5. Each plot area is 1 cm on a side.*

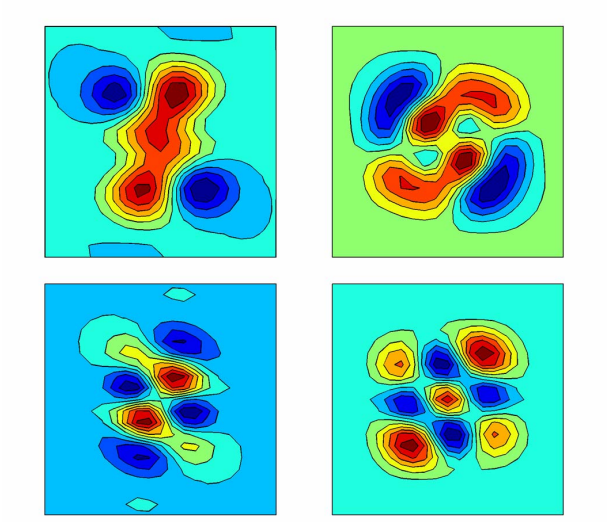

Figure 6. *The $u_1$ displacement component of the B-modes of Fig. 4. Each plot area is 1 cm on a side.*

The spread-out nature of these displacements helps couple vibrational energy of the B-mode to the outside world through the mounts and reduces the *Q*. This is the primary effect that allows suppression of the B-mode.

Since the calculated mode shapes from the variational model extend beyond the blank lateral dimensions, it is possible to calculate the displacement present around the perimeter of the blank for the different modes. Since the *Q* of a mode is affected by motional energy loss to the mounts, an estimate of the *Q* of a mode can be made by calculating the integral of the square of the edge displacement for different modes. The C-mode is well-trapped, so a comparison is made here with the ratio of this integral for the B-mode compared to the C-mode. This has been done for the 3.6864 MHz model vs. *D* in Figure 7.

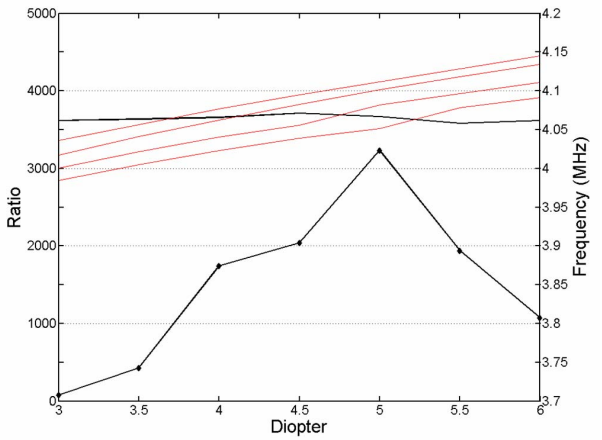


Figure 7. *Calculated ratio of the integral of the edge motion of the B-mode to the C-mode vs. D for the 3.6864 MHz blank design Frequency vs. D is included from Fig. 3 for reference..*

Note in Fig. 7 that this ratio starts at a very low value for the lowest *D* where the B-mode is well trapped (see Fig. 4), increases dramatically across the *D* range where the C-mode anharmonics are interacting, and decreases at large D where the B-mode is again relatively well defined (see Fig. 4). This effect helps suppress the B-mode over a wide temperature range.

## *C. Finite element modeling*

Since the variational modeling does not take into account the blank edges, finite element modeling, FEA, was used to assess the effects of blank edges. The Algor software was used [10]. Figure 8 shows the model for the 3.6864 MHz blank design. Sixteen linear sections were used to approximate a round blank. Also, the modeling used elements with fixed dimensions in the $x_1$ and $x_3$ (*x* and *z*) directions to facilitate numerical integration in post-processing.

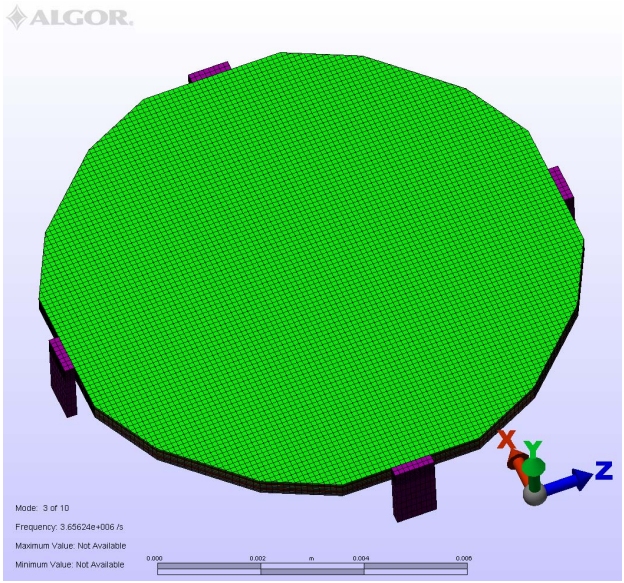


Figure 8. *Finite element model for the3.6864 Hz blank design.*

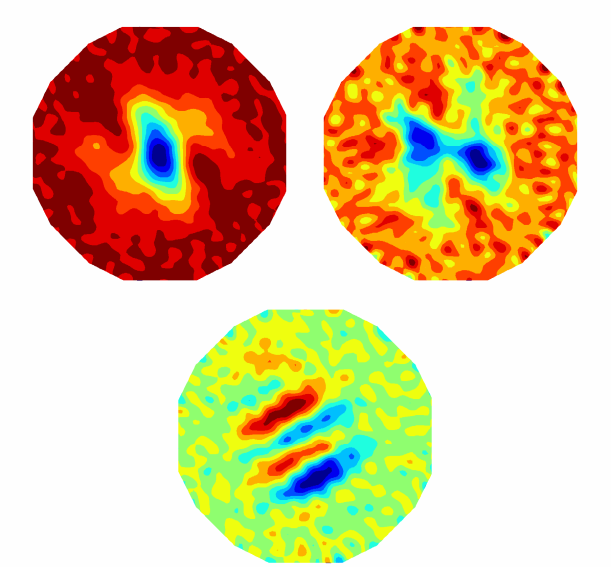

Figure 9. *FEA mode shape for $u_3$ for a 3.6864 MHz blank design with a D of 5 (compare to Fig. 5).*

One of the first things noted in comparing the FEA results to the variational results was that the sequence of the modes with increasing frequency was somewhat altered when approaching the B-mode frequency area. Even so, the mode shapes noted in Figs. 4-6 were very similar. As an example, Fig. 9 shows the FEA mode shapes for the $u_3$ displacement of the 3.6864 MHz blank design for a $D$ of 5, a direct comparison for the variational results shown in Fig. 5. Note the similarity of the mode shapes. The FEA results include flexural motion in the blank, which is seen in Fig. 9. Apparently, the major impact of the presence of the blank edges is some shifting of the frequencies of the $m + p = 4$ C-mode anharmonics and the subsequent perturbation of the frequency of the B-mode-like modes.

## III. Experimental Results

### A. Measurement equipment and samples

Measurements of various blank designs were done with a Saunders & Associates 2200 test chamber over a temperature range of 30 to 150°C. Frequency and resistance were measured for the C-mode ($C_{100}$), the B-mode ($B_{100}$), and the strong C-mode anharmonic ($C_{102}$).

The 3.6864 MHz design blanks were mounted on TO-8 headers with conducting polyimide and subsequently cold-welded with cans. Experiments involved groups of units, most results are presented as the average of the group.

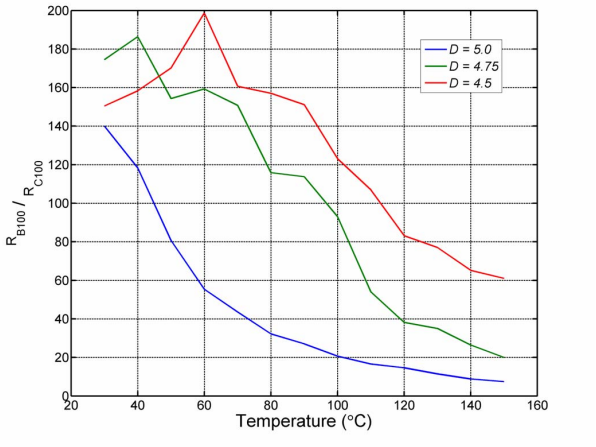


Figure 11. *Ratio of B-mode to C-mode resistances for the 3.6864 MHz blank design for D=4.5, 4.75, and 5.0.*

### B. Results for the 3.6864 MHz blank design

This blank design was studied in detail. Figure 11 shows the ratio of B-mode to C-mode resistances vs. $T$ for three different $D$ values. The data in Fig. 11 are the average of 24, 20, and 14 units for $D$ = 4.5, 4.75, and 5.0, respectively. As discussed above, increasing $T$ moves the B-mode frequency down relative to the C-mode anharmonics, which is the same as increasing $D$ (see Fig. 2). Thus, decreasing the $D$ of the blank design moves the B-mode deeper into the cluster of C-mode anharmonics, causing a more degraded $Q$ and resistance over a larger temperature range.

The frequency of the $C_{102}$ C-mode anharmonic is a measure of the $D$ of the blank. Figure 12 shows the frequency vs. $T$ for the 3.6864 MHz design for all units studied. First of all, note that the groups are well defined for each $D$ value. This lends credibility to the separation of the averages shown in Fig. 11. In addition, measurement of the $C_{102}$ frequency provides a ready quality control on production.

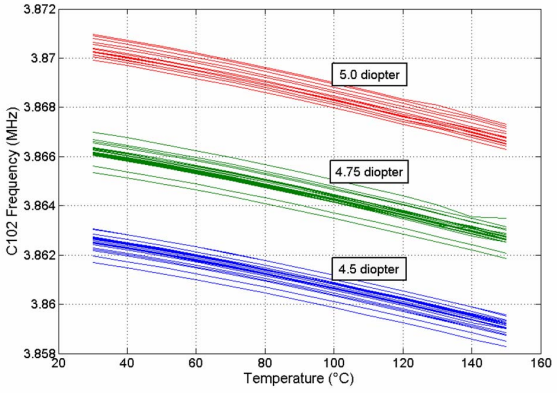


Figure 12. *Measured frequencies of the $C_{102}$ C-mode anharmonic vs. T for the 3.6864 MHz blank design for D=4.5, 4.75, and 5.0.*

## IV. CONCLUSIONS

It has been shown that the fundamental B-mode can be adequately suppressed in a plano-convex blank by judicious choice of blank diopter. The suppression comes from strong interaction of the B-mode with a family of C-mode anharmonics. The theoretical basis for the effect is supported by three different approaches. Analytical modeling of the modes provides the general range of desirable *D* values, but does not predict the physical interaction between the B-mode and the C-mode. Variational modeling shows the interaction and provides information about distorted mode shapes and increased vibrational motion of the B-mode around the blank perimeter, which degrades the mode *Q*. Finite Element Analysis demonstrates that the effects of finite blank dimensions and presence of mounts slightly alters the sequence of modes with increasing frequency, but demonstrates that the B-mode has distorted shapes arising from the coupling to the C-mode anharmonics.

The experimental results support the theoretical results and lead to practical blank design criteria for crystals that can be used over a wide temperature range with the B-mode suppressed sufficiently to avoid inductors in the circuitry.

## REFERENCES


[1] E. P. EerNisse, "Quartz resonator frequency shifts arising from electrode stress, Proc. 29th Annual Symposium on Frequency Control, p. 1, 1975

[2] J. Kusters, "Transient thermal compensation for quartz resonators," IEEE Trans. Sonics and Ultrasonics, SU-23, pp. 273-276, July 1976.

[3] Raymond L. Filler and John R. Vig, "Fundamental mode SC-cut resonators," Proc. 34th Annual Symposium on Frequency Control, p. 187, 1980.

[4] E. P. EerNisse, "Resonant mode calculations of contoured doubly-rotated quartz crystals using a variational approach," Proc. 2003 IEEE Ultrasonics Symposium, p. 1432, 2003.

[5] D. S. Stevens and H. F. Tiersten, "An analysis of doubly rotated quartz resonators utilizing essentially thickness modes with transverse variation," J. Acoust. Soc. Am., Vol. 79, p. 1811, 1986.

[6] E. P. EerNisse, "Analysis of thickness modes of contoured, doubly rotated, quartz resonators," IEEE Trans. Ultrasonics, Ferroelectrrics, and Freq. control, Vol. 48, p. 1351, 2001.

[7] Bikash K. Sinha, "Doubly rotated contoured quartz resonators," IEEE Trans. Ultrasonics, Ferroelectrrics, and Freq. control, Vol. 48, p. 1162, 2001.

[8] E. P. EerNisse, Design of Resonant Piezoelectric Devices, Cambridge: The M.I.T. Press, 1969.

[9] B. Dulmet, "A general model for quasi-thickness vibrations in contoured plates," Proc. 5th Europ. Freq. and Time Forum, Besancon, France, 1991.

[10] See Algor.com.